

Figure 2: Imaginary part versus real part of  $\Gamma^*$  (blue) and  $\Gamma$  (red).

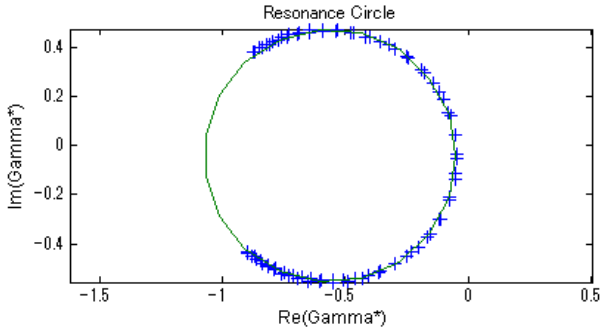


Figure 3: Imaginary part versus real part of  $\Gamma^*$ : Measured data (blue) and fit (green).

where  $c$  and  $r$  result from a fit of a circle to the measured data (see Figure 3). The point  $\Gamma_\infty^*$  corresponds to  $(-1, 0)^T$  in reality, which allows the normalization

$$\frac{d}{a} = -\frac{1}{\Gamma_\infty^*} . \quad (6)$$

Insertion of this in equation (3) and in equation (1) yields the reconstructed cavity signal.

Once the calibration factor  $d/a$  is determined and set to the system,  $U_{cav}$  is calculated in real-time. Thereby a stable feedback operation was established yielding a longtime stability of  $\Delta A/A_{RMS} = 0.094\%$  in amplitude and  $\Delta\phi_{RMS} = 0.056^\circ$  in phase, respectively. Figures 4 and 5 are showing amplitude and phase of the respective pulse.

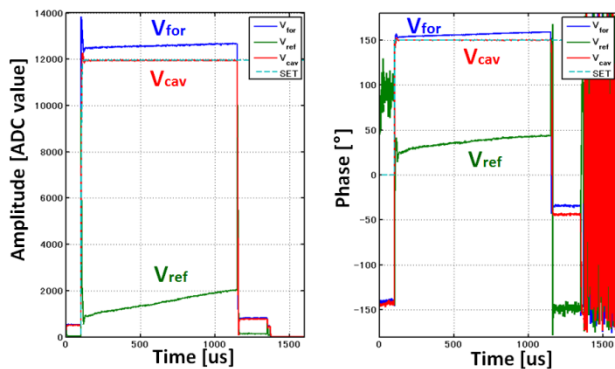


Figure 4: Amplitude (left) and phase (right) versus time of the forward signal (blue), the reflected signal (green), the reconstructed cavity signal (red), and the set point (light blue) of an RF pulse while feedback operation.

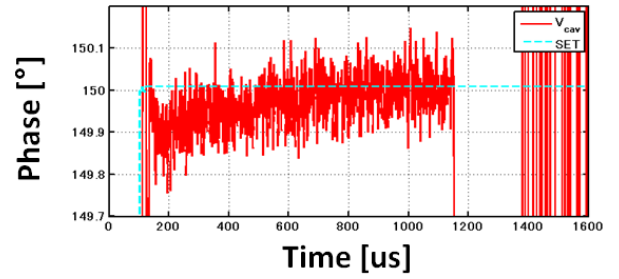
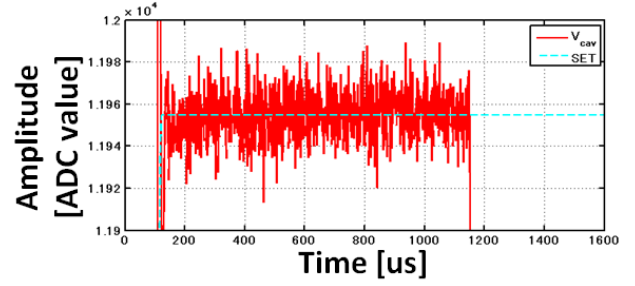


Figure 5: Zoomed in region of amplitude (top) and phase (bottom) at first flattop versus time of reconstructed cavity signal (red) and set point (light blue) during feedback operation.

Beside this the calibration method allows to obtain the coupling coefficient  $\beta$  by

$$\beta = \frac{1+\Gamma_0}{1-\Gamma_0} . \quad (7)$$

## BEAM-BASED CALIBRATION OF SUPERCONDUCTING CAVITIES

As shown in Figure 6 the DRFS waveguide system consists beside others of several waveguide phase shifters (WPS) and waveguide reflectors (WR). Thereby the combination of WR 1 and WPS 3 as well as WR 2 and WPS 4 are used to set the  $Q_L$  values of cavity 1 (MHI 12) and cavity 2 (MHI 13), respectively [7].

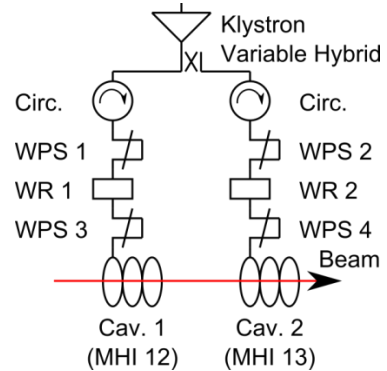


Figure 6: Schematic of the DRFS waveguide system: Klystron, variable hybrid, circulators, waveguide phase shifters (WPS 1 and WPS 2), waveguide reflectors (WR 1 and WR 2), waveguide phase shifters (WPS 3 and WPS 4), and superconducting cavities (MHI 12 and MHI 13).

By scanning the RF phase using WPS 1 and WPS 2 consecutively while observing the beam induced change in amplitude  $\Delta A$  at the flattop of the pulses [8] as shown in Figure 7 for each cavity the RF phases for on-crest beam acceleration were determined.

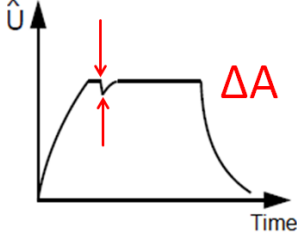


Figure 7: Amplitude versus time of an RF pulse including a beam induced drop-off during the flat top.

Those correspond to the maximal negative  $\Delta A$  and are identified by a fitting procedure. By taking the charge per bunch into account as well as averaging over ten pulses per step motor position, the calibration method was improved so that the fluctuation due to the change of the charge per bunch over time could be smoothed out. Figure 8 shows a respective phase scan. Besides determining the RF phases the loop phase for the feedback loop was set to zero and a reference table was created, which allowed a stable feedback operation.

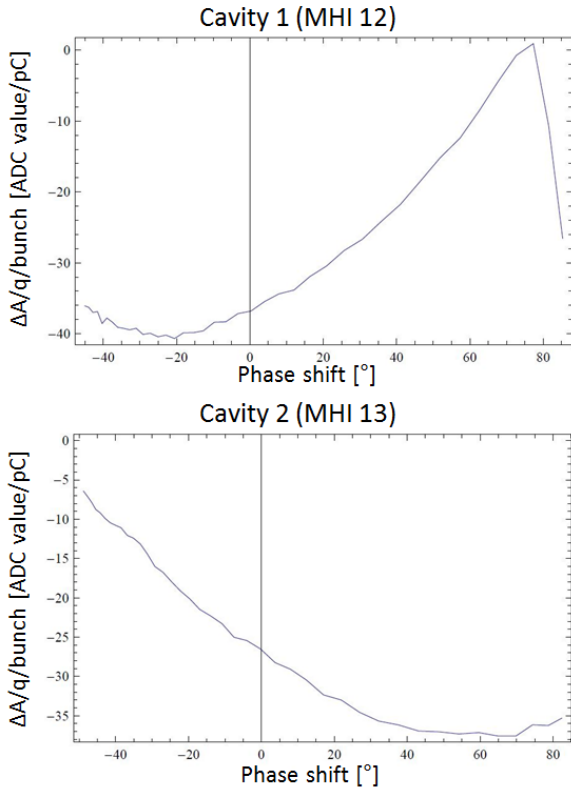


Figure 8: Beam induced amplitude  $\Delta A$ /charge per bunch versus RF phase shift for cavity 1 (top) and cavity 2 (bottom). The drop at cavity 1 above  $77^\circ$  of RF phase shift originates from effects of far off-crest beam operation.

In a low power measurement of the two paths between the klystron and the two cavities in the DRFS waveguide system (see Figure 6) after a RF phase shift calibration it was shown that the phase difference between the two cavities is  $\varphi_{\text{cav1cav2}} = 93^\circ$ . Since the cavities are mounted in  $\lambda/4$  distance the measured value is in good agreement with the expected and required value of  $90^\circ$ , showing that the developed and applied method is effective.

The beam induced voltage, which causes to a drop in amplitude as shown in Figure 9 for five different step motor positions of WPS 1, can be calculated by

$$\Delta V_{\text{ind}} = I_b \cdot \Delta t \cdot \frac{r}{Q} \cdot \pi \cdot f_0 \quad (8)$$

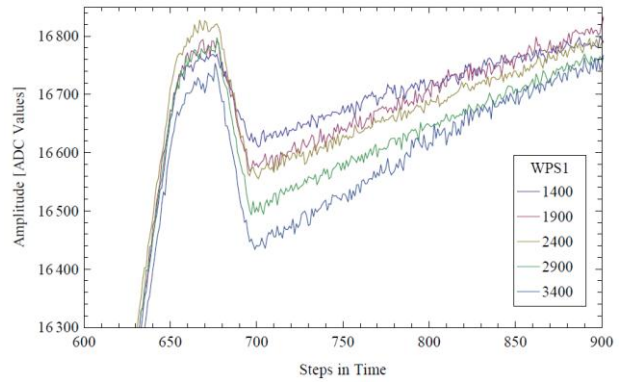


Figure 9: Zoomed in region of amplitude versus steps in time of flattop including beam for five different WPS 1 step motor positions.

Comparing this value with the ADC values allows a calibration of those. Taking the length of the cavities into account yielded cavity gradients of  $V_{\text{cav1}} = 18.7 \text{ MV/m}$  and  $V_{\text{cav2}} = 19.2 \text{ MV/m}$ . The errors for these values due to the calibration method are  $\Delta V_{\text{cav1}} = 4.8\%$  and  $\Delta V_{\text{cav2}} = 4.9\%$ . In respect of the estimated errors, these cavity gradients are in good agreement with the measured beam energy of 40 MeV.

## SUMMARY

By developing and applying a calibration method for the forward and reflected signal in the waveguide of the STF RF gun, the cavity signal could be reconstructed, which allowed a stable feedback operation even in absence of an actual pick-up antenna with a longtime stability of  $\Delta A/A_{\text{RMS}} = 0.094\%$  in amplitude and  $\Delta \phi_{\text{RMS}} = 0.056^\circ$  in phase, respectively.

A beam-based calibration method for the RF phase for on-crest acceleration as well as for the cavity gradients was developed and successfully applied. The determined cavity gradients were  $V_{\text{cav1}} = 18.7 \text{ MV/m}$  and  $V_{\text{cav2}} = 19.2 \text{ MV/m}$  with an error of  $\Delta V_{\text{cav1}} = 4.8\%$  and  $\Delta V_{\text{cav2}} = 4.9\%$  due to the calibration method. Furthermore the stable feedback operation of the DRFS system was achieved.

## REFERENCES

- [1] <http://www.linearcollider.org>
- [2] H. Hayano, "Status of Superconducting RF Test Facility (STF)", Presentation, The 9<sup>th</sup> Annual Meeting of Particle Accelerator Society of Japan, Toyonaka, 2012, THPS096.
- [3] S. Fukuda, "Distributed RF Scheme (DRFS) – Newly Proposed HLRF Scheme for ILC", Proceedings of Linear Accelerator Conference LINAC2010, Tsukuba, 2010, MOP027.
- [4] T. Miura et al., "Performance of the  $\mu$ TCA Digital Feedback Board for DRFS Test at KEK-STF", Proceedings of IPAC2011, San Sebastián, 2011, MOPC155.
- [5] S. Michizono et al., "Performance of LLRF System at S1-Global in KEK", Proceedings of IPAC2011, San Sebastián, 2011, MOPC157.
- [6] A. Brandt, "Development of a Finite State Machine for the Automated Operation of the LLRF Control at FLASH", Doctoral Thesis, Universität Hamburg, Hamburg, 2007.
- [7] S. Kazakov et al., "L-band Waveguide Elements for SRF Application", Proceeding of Particle Accelerator Society Meeting, Tokai, 2009, FPAC22.
- [8] M. Liepe, „Regelung supraleitender Resonatoren mit Strahlbelastung am TESLA-Test-Linearbeschleuniger“, Diploma Thesis, Universität Hamburg, Hamburg, 1998.